Published in final edited form as:

Cancer Res. 2016 November 1; 76(21): 6362–6373. doi:10.1158/0008-5472.CAN-16-1306.

Histone H3K27 trimethylation modulates 5-fluorouracil resistance by inhibiting PU.1 binding to the DPYD promoter

Rentian Wu[1], **Qian Nie**[1], **Erin E. Tapper**[1], **Calvin R. Jerde**[1], **Garrett S. Dunlap**[1], **Shikshya Shrestha**[1], **Tarig A. Elraiyah**[1,2], **Steven M. Offer**[1,2,*,3], and **Robert B. Diasio**[1,2,*,3]

[1]Department of Molecular Pharmacology and Experimental Therapeutics, Mayo Clinic Cancer Center, 200 1st St SW, Rochester, MN 55905, USA

[2]Mayo Clinic College of Medicine, Mayo Clinic, 200 1st St. SW, Rochester, MN, 55905, USA

Abstract

The antimetabolite 5-fluorouracil (5-FU) is one of the most widely used chemotherapy drugs. Dihydropyrimidine dehydrogenase (DPD) is a major determinant of 5-FU response and toxicity. While *DPYD* variants may affect 5-FU metabolism, they do not completely explain the reported variability in DPD function or the resultant differences in treatment response. Here, we report that H3K27 tri-methylation (H3K27me3) at the *DPYD* promoter regulated by Ezh2 and UTX suppresses *DPYD* expression by inhibiting transcription factor PU.1 binding, leading to increased resistance to 5-FU. Enrichment of H3K27me3 at the *DPYD* promoter was negatively correlated with both *DPYD* expression and DPD enzyme activity in peripheral blood specimens from healthy volunteers. Lastly, tumor expression data suggests that *DPYD* repression by Ezh2 predicts poor survival in 5-FU-treated cancers. Collectively, the findings of the present manuscript suggest that a previously uncharacterized mechanism regulates DPD expression and may contribute to tumor resistance to 5-FU.

Keywords

Histone H3K27me3; Ezh2; UTX; dihydropyrimidine dehydrogenase; 5-fluorouracil response

Introduction

Two major obstacles that limit the effectiveness of chemotherapy are low response rates and the high degree of treatment-associated toxicities. As one of the most widely used chemotherapeutics, the antimetabolite 5-fluorouracil (5-FU) confronts the same issues. When administered as a single agent, the response rate for 5-FU is usually less than 20% (1). The addition of other drugs (i.e., combination chemotherapy) can improve response rates to as high as 50%; however, this improvement in efficacy is often accompanied by a dramatic increase in adverse toxicity (2, 3). Therefore, a better understanding of the mechanisms that contribute to drug resistance and toxicity has the potential to improve treatment efficacy.

*Correspondence: diasio.robert@mayo.edu (R.B.D.), offer.steven1@mayo.edu (S.M.O.).
[3]Co-senior author

The authors have no conflict of interest to disclose.

Dihydropyrimidine dehydrogenase (DPD, encoded by *DPYD*) catabolizes 85% of administered 5-FU to the non-toxic metabolic intermediate 5-dihydrofluorouracil (4). Specific *DPYD* variants have been shown to impair DPD enzymatic activity *in vitro* (5) and significantly increase the risk of 5-FU toxicity *in vivo* (6). However, known SNPs only account for approximately 30% of cases of severe toxicity to 5-FU (7, 8), and the majority of patients who develop 5-FU toxicity do not carry known toxicity-associated *DPYD* SNPs (6). In addition to genetic variation in *DPYD*, differences in *DPYD* expression have been reported in cancer patients (9, 10). A limited retrospective study demonstrated that patients with low tumor expression of *DPYD* experienced higher response rates to 5-FU compared to patients with high tumor expression of *DPYD* (11). Collectively, these observations suggest that the regulation of *DPYD* expression in both normal and tumor tissues controls 5-FU catabolism and response. Therefore, *DPYD* transcriptional control is paramount to the sensitivity and resistance to 5-FU.

Gene expression is known to be epigenetically regulated by the methylation of DNA and/or by the modification of histones. Tri-methylation of lysine 27 on histone H3 (H3K27me3) acts to repress gene expression (12). Changes in H3K27me3 are frequently observed in cancer (13). Additionally, inactivating somatic mutations in the H3K27me3 demethylase *UTX* have been identified in diverse cancers, including multiple myeloma, esophageal, renal, and bladder cancers (14). Mutations in, or overexpression of, the H3K27me3 methyl-transferase *EZH2* have also been observed in various cancers, including leukemia, prostate, breast, lung, and liver cancers (15).

In this manuscript we present a previously unrecognized mechanism contributing to 5-FU toxicity and sensitivity. We demonstrate that *DPYD* expression is directly regulated by the histone H3K27me3 methyl-transferase Ezh2 and the demethylase UTX. H3K27me3 inhibits PU.1 binding, decreasing *DPYD* expression and increasing 5-FU sensitivity. Tumors with high *DPYD* and low *EZH2* expression are significantly more resistant to 5-FU–based therapy, strongly suggesting that H3K27me3 at the *DPYD* promoter may be a robust predictive biomarker for 5-FU response.

Material and Methods

Cell lines

Low-passage HEK293T/c17 (ATCC CRL-11268), Hela (ATCC CCL-2), HepG2 (ATCC HB-8065), HCT116 (ATCC CCL-247), RKO (ATCC CRL-2577), SW480 (ATCC CCL-228), SW620 (ATCC CCL-227) and HT-29 (ATCC HTB-38) cells were obtained from the American Type Culture Collection (ATCC) in 2013 and maintained at 37°C in a humidified incubator with an atmosphere of 5% CO_2. Cells were cultured using DMEM (Mediatech) supplemented with 10% FBS (Denville Scientific), penicillin and streptomycin (Mediatech).

Antibodies and primers

Antibodies were used as following: Histone H3 (WB 1:5000) was a generous gift from Dr. Zhiguo Zhang; anti-DPD (ab6556, WB 1:2000), TS (ab58287, WB 1:2000) and Tubulin

(ab186407, WB 1:5000) were purchased from Abcam; H3K27me3 (C36B11, WB 1:5000) and Ezh2 (D2C9, WB 1:2000) were purchased from Cell Signaling Technology; PU.1 (sc-352 X, WB 1:1000) was purchased from Santa Cruz. Primers used for real-time PCR are list in Table S1.

Vector construction

To generate gRNA expression vectors, annealed oligonucleotides (Integrated DNA Technologies, listed in Table S2) were cloned into the lentiGuide-Puro vector, a gift from Dr. Feng Zhang, which was obtained from Addgene (plasmid #52963). The expression vector for dCas (plasmid #46910) was a gift from Stanley Qi & Jonathan Weissman. The lentiviral packaging vectors pMD2.G (plasmid #12259) and psPAX (plasmid #12260), were obtained from Addgene. Lentivirus vectors expressing shRNAs targeting PU.1 (sh1: TRCN0000426240; sh2: TRCN0000417534) and EZH2 (sh1: TRCN0000353069; sh2: TRCN0000286290) were obtained from Sigma-Aldrich. Wildtype and mutant histone H3 expression vectors were generous gifts from Dr. Zhiguo Zhang.

Chromatin immunoprecipitation

Chromatin immunoprecipitation assays were performed as described (16) with minor changes. Cells were fixed with 1% formaldehyde for 10 min at room temperature and quenched with 125 mM glycine. Chromatin was sheared by sonication (Bioruptor Pico) to average lengths of 500 bp. Chromatin was immunoprecipitated using 10 μg relevant antibodies and protein A beads. DNA was recovered from the protein A complex using elution buffer (10 mM Tris, 10 mM EDTA, 1% SDS, 150 mM NaCl, 5 mM DTT, pH 8.0) and purified using Macherey-Nagel PCR Clean-up kit. The amount of specific DNA sequences recovered during each ChIP assay was quantified by real-time PCR.

Cell viability and Real-time cellular analysis

Cells were seeded at standardized concentrations to ensure sub-confluence at 48 hours after treatment. Drug treatments were applied 24 hours post-seeding. Viable was estimated using CellTiter-Blue (Promega) 48 hours after treatment. Real-time cellular analysis using the xCELLigence RTCA system (Acea Biosciences) was performed as described (5).

Healthy volunteer specimens

Healthy volunteers that did not carry the known deleterious *DPYD* variants rs3918290, rs55886062, or rs67376798 (6) were identified using the Mayo Clinic Center for Individualized Medicine Biobank (17). DPD enzyme activity was measured in PBMC lysates as previously described (18). RNA was extracted from PAXgene Blood RNA Tubes (Becton Dickinson) using the PAXgene Blood RNA kit (Qiagen) using standard protocols. All participants provided informed consent for these studies, which were approved by our institutional review board.

Transcription factor binding site prediction

The promoter region of *DPYD* (1.5 kb upstream of transcription start site) was analyzed by PROMO (19) using version 8.3 of TRANSFAC transcription factor database with random expectation value threshold set to <0.005.

Statistical analyses

RNA-seq data for individual TCGA cancer types (Illumina HiSeqV2, version 2015-02-24, RSEM normalized) and all clinical information were retrieved using the UCSC Cancer Browser. A cohort of colorectal cancer patients with known treatment information was obtained from publically available data set GSE40967. Standard scores (z-scores) of log2 transformed normalized read counts were calculated for expression analyses. Pearson's correlations, Kaplan-Meier plots, and Cox proportional-hazards regression analyses were performed using R version 3.2.3. IC_{50} and two-tailed Student's t-tests were calculated using GraphPad Prism6.

Results

Identifying *EZH2* as a potential regulator of *DPYD* expression

To identify potential pathways through which *DPYD* could be regulated, we screened expression data from The Cancer Genome Atlas (TCGA) for correlations between epigenetic regulatory genes and *DPYD* gene expression. Overall, *DPYD* expression was significantly reduced in tumor samples compared to normal tissues for various cancers, including colon, gastric, and breast cancers (Figure 1A; *DPYD* expression data for additional cancer types is shown in Figure S1A). In contrast, expression of the H3K27 methyl-transferase *EZH2* was significantly elevated in colon, gastric, and breast tumors (Figures 1A; data for additional cancers is shown in Figure S1A). The expression of *EZH2* showed negative correlation with *DPYD* expression in both tumor (Figures 1B and S1B) and normal (Figure 1C) tissues. To further address the link between Ezh2 and *DPYD*, we treated HEK293T cells, which we previously showed express undetectable levels of DPD (5), with various chemical inhibitors directed against the major histone modification enzymes that control transcription. The greatest increase in *DPYD* expression was noted for cells treated with GSK-126 (Figure S1C), a highly selective small molecule inhibitor of Ezh2 that has been shown to inhibit global H3K27 tri-methylation (20).

It is widely recognized that the epigenetic landscape in tumor cells differs greatly from that of normal cells. Therefore, we tested for correlations between expression in tumor and matched normal tissues for *DPYD* and *EZH2*. The expression of neither gene showed evidence for correlation between tumor and normal tissues (Figure S1D), suggesting that the regulation of both genes in tumors is independent from their regulation in normal tissues.

Inhibition of Ezh2 increases *DPYD* gene expression

Based on the correlations observed in TCGA data, we hypothesized that H3K27 tri-methylation by Ezh2 would repress *DPYD* expression. Therefore, inhibition of Ezh2 would be expected to increase *DPYD* levels. To test this hypothesis, various cell lines were treated with GSK-126. As previously reported, global levels of H3K27me3 were reduced in all cell

types treated with GSK-126 (Figure 2A and S2A). Additionally, GSK-126 significantly increased *DPYD* expression in HEK293T, HCT116, SW480, SW620 and RKO cells, but not Hela cells (Figure 2B and S2B). Knocking down *EZH2* by specific shRNA showed similar effect in HEK293T, HCT116, HT29 and Hela cells. (Figures S2C and S2D). Dose- and time-dependent increases of *DPYD* expression following GSK-126 treatment were noted using HEK293T (Figures 2C and 2D) and HCT116 cells (Figures S2E and S2F).

To confirm the results obtained by using the chemical inhibitor GSK-126, we generated cell lines that express a lysine 27 to methionine mutant version of histone H3 designated herein as H3K27M that originally been detected in pediatric glioblastomas (K27M) (21, 22), which inhibited global tri-methylation levels of H3K27 in heterozygous carriers in a strongly dominant-negative manner (16, 23, 24). As expected, cells that stably expressed H3K27M showed significant reductions in global H3K27me3 levels, but no overall change in H3 expression (Figure 2E and S2G). For the colorectal tumor lines HCT116, HT29, and SW480, but not Hela cells, DPD protein expression was elevated in H3K27M-expressing cells compared to matched wildtype cells (Figure 2E and S2G). With the exception of Hela cells, *DPYD* expression was significantly higher in cells expressing H3K27M (Figure 2F and S2H). Additionally, the IC_{50} for 5-FU was significantly increased in H3K27M expressing cells compared to cells expressing wildtype H3 for all cell lines tested (Figure 2G). Taken together, these results corroborated the observations from the chemical inhibition of Ezh2 with GSK-126 and strongly suggest that *DPYD* expression is suppressed by Ezh2.

Thymidylate synthetase (TS, encoded by *TYMS*) is the other major gene that has been suggested to contribute to 5-FU resistance and response (25). No significant changes in *TYMS* expression were noted for cells treated with GSK-126 (Figure S2I) or for cells stably expressing H3K27M (Figure S2J).

Promoter enrichment of Ezh2 and H3K27me3 correlates with *DPYD* expression

To determine if Ezh2 and H3K27me3 were enriched on the *DPYD* promoter of cells expressing low levels of *DPYD*, chromatin immunoprecipitation (ChIP) was performed using antibodies against Ezh2 and H3K27me3. The region that was examined included the promoter, the transcription start site (TSS), and the first two exons (Figure 3A). Ezh2 and H3K27me3 were highly enriched on the *DPYD* promoter and exon 1 in RKO, HEK293T and SW480 cell lines (Figure 3B), which expressed the lowest levels of *DPYD* (Figure 3C). Ezh2 and H3K27me3 were moderately enriched on the *DPYD* promoter in HepG2 and HCT116 cells; almost no enrichment was noted in Hela and HT29 cell lines (Figure 3B). The localized enrichment of H3K27me3 could be reversed using GSK-126 (Figure 3D).

We estimated the cumulative Ezh2 and H3K27me3 ChIP enrichment at the *DPYD* promoter and Exon1 (i.e., from −2 kb to +1 kb from the TSS; Figure 3A) to determine correlation with *DPYD* expression (Figure 3E). ChIP enrichment of Ezh2 and H3K27me3 were highly correlated (r=0.97, p=0.0003). *DPYD* expression was negatively correlated with both Ezh2 and H3K27me3 accumulation (Ezh2: r=−0.93, p=0.0024; H3K27me3: r=−0.96, p=0.0006). These data support our hypothesis that the level of Ezh2 and H3K27me3 could explain the difference in *DPYD* gene expression between various different cell lines.

Inhibiting the demethylases UTX and Jmjd3 decreases *DPYD* gene expression

We hypothesized that the H3K27-specific demethylases UTX and Jmjd3 (26) promote *DPYD* expression through removal of inhibitory H3K27me3 from the *DPYD* promoter. In TCGA RNA-seq data, *UTX* and *JMJD3* were positivity correlated with *DPYD* expression in colon cancer (Figure 4A), which is consistent with the negative correlation observed between *DPYD* and *EZH2* (Figures 1B and 1C). Expression of *UTX* and *JMJD3* are both reduced in tumor compare to normal tissues (Figure S3), whereas expression of *EZH2* was increased in tumors (Figure 1A).

To experimentally corroborate these findings, we suppressed demethylation of H3K27me3 using GSK-J4, an inhibitor of the catalytic sites of UTX and Jmjd3. Consistent with previous findings (27), we did not observe an overall change of H3K27me3 level in Hela and HCT116 cell lines (Figure 4B). GSK-J4 treatment significantly increased H3K27me3 ChIP enrichment at the *DPYD* promoter in HCT116 cells (Figure 4C). Dose-dependent reductions in DPD and *DPYD* expression were observed for both cell lines (Figures 4B and 4D).

To determine if induction of H3K27me3 enhances 5-FU anti-tumor activity *in vitro*, HCT116 cells were treated with 5-FU, GSK-J4, or a combination of 5-FU and GSK-J4. Cell viability was significantly impaired with treatment of GSK-J4 or 5-FU alone (Figure 4E). The decrease in viability was more pronounced in cells treated with both GSK-J4 and 5-FU (Figure 4E), suggesting that H3K27 demethylation enhances 5-FU efficacy by up-regulating DPD.

H3K27me3 at the *DPYD* promoter inhibits transcription factor PU.1 binding

Six candidate transcription factor binding sites in the *DPYD* promoter were identified using PROMO (19). *SPI1*, which encodes for PU.1, showed the strongest correlation with *DPYD* expression in colorectal (Figures 5A, 5B, and S4A) and other (Figure S4B) tumor types in the TCGA dataset. In cellular studies, PU.1 knockdown significantly reduced DPD expression (Figure 5C). It is noted that *DPYD* promoter-specific PU.1 enrichment varied between cell lines (Figure S4C). Both PU.1 enrichment and Ezh2 or H3K27me3 enrichment on the *DPYD* promoter were negatively correlated, whereas PU.1 ChIP enrichment on the *DPYD* promoter positively correlated with *DPYD* expression (Figure 5D).

Given the negative correlation between PU.1 and H3K27me3 ChIP enrichment (Figure 5D), we hypothesized that changing the H3K27 tri-methylation level would alter PU.1 binding affinity. GSK-126 significantly increased PU.1 enrichment on the *DPYD* promoter, whereas GSK-J4 showed the opposite effect (Figure 5E). These data, combined with the decrease and increase in H3K27me3 levels measured after GSK-126 and GSK-J4 treatments (Figures 3D and 4C), respectively, strongly suggest that tri-methylation of H3K27 at the *DPYD* promoter regulates transcription by inhibiting PU.1 binding.

Promoter-specific targeting of Ezh2 or UTX alters *DPYD* expression and cellular sensitivity to 5-FU

Modified CRISPR methodology was utilized to manipulate H3K27me3 levels specifically at the *DPYD* promoter. Briefly, a nuclease-deficient Cas9 (dCas9) protein, was fused to either

Ezh2 or UTX and expressed in various cell lines together with guide RNAs (gRNAs) that were designed to target different regions of the *DPYD* gene, including the promoter, TSS, or Exon1 (Figure S5A). To minimize potential artifacts that could be introduced from overexpressing Ezh2 or UTX, low levels of the fusion proteins were expressed that did not change the overall H3K27me3 level (Figure S5B).

Ezh2 and UTX targeting was confirmed using H3K27me3 ChIP-qPCR on cells co-expressing all six gRNAs. *DPYD* promoter H3K27me3 levels significantly increased in all dCas9-Ezh2–expressing cell lines compared to cells expressing dCas9 control (Figure 6A). H3K27me3 enrichment on the *DPYD* promoter decreased in all UTX-targeting cell lines (Figure 6A). Changes were restricted to the region of −7 kb to +7 kb of the *DPYD* TSS (Figure 6A and data not shown), in agreement with unchanged global H3K27me3 levels (Figure S5B).

In HEK293T cells, which possessed the highest level of H3K27me3 on the *DPYD* promoter (Figure 3B), targeting dCas9-Ezh2 to the *DPYD* promoter showed no effect on *DPYD* expression (Figure 6B), suggesting that the natural level of tri-methylation in this cell line may be adequate to effectively inhibit PU.1 binding. On the other hand, targeting dCas9-UTX to either the promoter or Exon1 greatly increased *DPYD* expression (Figure 6B). For HCT116 cells, which expressed moderate levels of *DPYD*, targeting dCas9-Ezh2 suppressed *DPYD* expression, while guiding dCas9-UTX to the promoter or Exon 1 increased *DPYD* expression (Figure 6C). In Hela cells, dCas9-Ezh2 inhibited *DPYD* expression when targeted to any of the regions surrounding the promoter, whereas dCas9-UTX increased *DPYD* expression only when targeted to the promoter and Exon1 (Figure 6D).

To determine the effect of *DPYD*-specific H3K27 tri-methylation and de-methylation on 5-FU sensitivity, we treated cell lines co-expressing promoter-targeted gRNAs and dCas9, dCas9-Ezh2, or dCas9-UTX with various concentrations of 5-FU. Targeting of dCas9-Ezh2 to the *DPYD* promoter increased 5-FU resistance in Hela, HCT116, and HEK293T cells (summarized in Figure 6E–G; representative images are shown in Figure S5C). Guiding dCas9-Ezh2 to the *DPYD* promoter caused Hela and HCT116 cells, but not HEK293T cells, to be more sensitive to 5-FU treatment (Figure 6E–G and S5C). These findings are consistent with the changes in *DPYD* expression noted for the various cell lines expressing promoter-guided dCas9-Ezh2 or dCas9-UTX (Figures 6B–D).

To further characterize the effects on 5-FU sensitivity, the IC_{50} for 5-FU was measured (Figure 6H–J). Targeting of dCas9-Ezh2 to the *DPYD* promoter did not significantly affect the IC_{50} for 5-FU in HEK293T cells (4.8 μmol/L for dCas9-UTX compared to 4.6 μmol/L for dCas9 control; $p = 0.97$); however, targeting of dCas9-UTX significantly increased the IC_{50} (32.2 μmol/L; $p = 1.5\times10^{-3}$). The lack of effect noted when Ezh2 is targeted to the *DPYD* promoter can be explained by the high level of H3K27me3 on the *DPYD* promoter in HEK293T cells (Figure 3A). The IC_{50} for 5-FU in Hela cells expressing dCas9 was 38.9 μmol/L. Targeting of dCas9-UTX to the promoter significantly increased the IC_{50} (174 μmol/L; $p = 6.7\times10^{-6}$), and targeting dCas9-Ezh2 significantly reduced the IC_{50} (20 μmol/L; $p = 1.7\times10^{-4}$). Similar changes were noted in HCT116 cells, for which the IC_{50} for dCas9 was 2.9 μmol/L, dCas9-UTX was 8.9 μmol/L ($p = 3.6\times10^{-4}$), and dCas9-Ezh2 was 1.3

μmol/L (p =1.1×10^{-4}). Collectively, these results demonstrate that anchoring Ezh2 or UTX to the *DPYD* promoter specifically alters local H3K27me3 levels, *DPYD* gene expression, and 5-FU sensitivity/resistance.

Use of Ezh2 and H3K27me3 levels as predictive biomarkers of 5-FU sensitivity/resistance

To assess the relationship between *DPYD* and H3K27me3 levels and tumor resistance to 5-FU, we analyzed overall survival and relapse-free survival data following treatment with a 5-FU-containing regimen in a publically available colorectal cancer dataset GSE40967 (28) and in the TCGA data set for colorectal and gastric cancer patients. For the 20% of patients who had tumors with the highest *DPYD* expression, overall survival and relapse-free survival were significantly reduced compared to patients whose tumors had lower *DPYD* expression (Figure 7A–D). COX regression analysis showed that high *DPYD* expression associated with significantly shorter survival. The median survival for colorectal cancer patients in the GSE40967 dataset with tumors expressing low *DPYD* levels was 4060 days, compared to 840 days for patients with high tumor *DPYD* levels (HR=2.64, log-rank p=0.006; Figure 7A). The median relapse-free survival for patients in the GSE40967 dataset with tumors expressing high tumor *DPYD* levels was 560 (note that fewer than 50% of low tumor *DPYD* level patients had died during the follow-up period; HR=2.36, log-rank p=0.015; Figure 7B). The median overall survival for colorectal cancer patients in the TCGA dataset with tumors expressing low *DPYD* levels was 2003 days, compared to 758 days for patients with high tumor *DPYD* levels (HR=4.26, log-rank p=0.0072; Figure 7C). The median overall survival for gastric cancer patients with tumors expressing low *DPYD* levels was 1294 days, while median survival for patients with high tumor *DPYD* expression was 712 days (HR=2.56, log-rank p=0.0066; Figure 7D).

Because we noted an inverse correlation between tumor expression of *DPYD* and *EZH2* (Figure 1B), we sought to determine if the addition of *EZH2* expression improved prediction of survival. In 5-FU-treated patients, a combination of high *DPYD* and low *EZH2* expression was significantly associated with shorter survival (Figure 7E–H) and served as a better predictor of survival than *DPYD* expression alone (Figure 7A–D). In the GSE40967 dataset, median overall survival improved from 784 to 4060 days (HR=4.3, log-rank p=5.02×10^{-5}; Figure 7E). Similarly, median relapse-free survival was also significantly different between the two groups (HR=4.10, log-rank p=7.38×10^{-5}; Figure 7F). Comparable results were noted in TCGA datasets for colorectal cancer (HR=5.99; log-rank p=3.1×10^{-4}; Figure 7G) and gastric cancer (HR=5.61; log-rank p=5.78×10^{-5}, Figure 7H). It is notable that stratification by *EZH2* expression alone did not yield significant differences in survival in any of the datasets analyzed (Figure S6 A–D).

To determine if H3K27me3 could also serve as a biomarker for *DPYD* expression in normal tissues, and thus as a potential predictor for severe 5-FU toxicity risk, we measured H3K27me3 on the *DPYD* promoter, *DPYD* expression, DPD enzyme activity, and *SPI1* expression in peripheral blood mononuclear cells (PBMCs) from healthy volunteers. *DPYD* expression was positively correlated with DPD enzyme activity (r=0.28, p=0.0085; Figure 7I). Negative correlations with H3K27me3 ChIP enrichment on the *DPYD* promoter were noted for both *DPYD* expression (r=-0.37, p=4.1×10^{-4} Figure 7J) and DPD activity

(r=-0.37, p=2.8×10^{-4} Figure 7K). Consistent with observations from the TCGA datasets (Figure 5B and S4B), *SPI1* positively correlated with both *DPYD* expression (r=0.86, p=4.3×10^{-16}; Figure 7L) and DPD activity (r=0.23, p=0.34 Figure 7M).

Discussion

Our data demonstrate that promoter H3K27me3 regulates *DPYD* expression and likely represents a clinically relevant determinant of tumor response to 5-FU. Our results support a model (Figure 7N) wherein Ezh2 and UTX have opposing roles at the *DPYD* promoter by regulating the binding of transcription factor PU.1. Modifying global H3K27me3 using either chemical (GSK-126 or GSK-J4) or genetic (H3K27M) approaches effectively modulated PU.1 binding to the *DPYD* promoter, resulting in altered *DPYD* expression and 5-FU sensitivity. Additionally, using CRISPR/dCas9-mediated targeting of Ezh2 or UTX, we confirmed that these results are due to tri-methylation of H3K27 specifically at the *DPYD* promoter. The combination of high *DPYD* and low *EZH2* expression in tumor cells was associated with poor outcome in 5-FU-treated colorectal and gastric cancer patients. Finally, the enrichment of H3K27me3 on the *DPYD* promoter was negatively correlated with cellular DPD activity and *DPYD* gene expression.

Our results strongly suggest that epigenetic repression of *DPYD* by H3K27me3 is a critical determinant of 5-FU resistance. Previous data have suggested that high *DPYD* expression associated with poor outcome following 5-FU treatment (9). Our findings further indicated that addition of tumor *EZH2* expression may help to further stratify patients based on the risk of tumor recurrence. This approach may help to identify patients that could benefit from aggressive adjuvant 5-FU chemotherapy. Specifically treatment options for stage II colorectal cancer patients represent a therapeutic challenge since limited benefit has been observed with adjuvant therapy in this group (29), despite a high risk of recurrence (30). Additional targeted studies of this association in stage II colorectal cancer may help direct therapeutic strategies justifying aggressive treatment in certain patients.

Ezh2 has been previously suggested to contribute to colorectal cancer development (31), but the role of Ezh2 in colorectal cancer recurrence or therapeutic response is largely unknown. Our data suggest that *EZH2* alone may have limited potential to predict outcome following 5-FU treatment in colorectal cancer (Figure S6), which is consistent with a previous report that showed a small to modest difference in outcome when patients were stratified by Ezh2 levels (31). Our data demonstrate that tumor *DPYD* expression may be a better predictor of outcome (Figure 7A–D), especially when combined with *EZH2* expression (Figure 7E–H). Collectively, these findings suggest that defects in Ezh2 (e.g., mutations) may disrupt the Ezh2-*DPYD* regulatory axis and affect 5-FU sensitivity. Inhibitors of Ezh2 or the KDM6 family (UTX and Jmjd3) have proven to be effective therapies for various cancers (27, 32–34). Ezh2 inhibitors have been shown to reverse drug-resistance in liver, brain, ovarian, and lung cancers (35–38), suggesting that the H3K27me3 epigenomic landscape may contribute to chemotherapy response. In the present study, our finding that Ezh2 regulates cellular response to 5-FU by inhibiting *DPYD* expression is perhaps unexpected based on a previous report that suggested that Ezh2 inhibition may sensitize tongue cancer cells to 5-FU (39). However, we confirmed our findings using multiple approaches including chemically

inhibiting H3K27me3 demethylation using GSK-J4, as well as using genetic approaches by expressing the dominant negative H3K27M mutant. Additionally, we demonstrate that the 5-FU response was due to direct modulation of H3K27me3 at the *DPYD* promoter using dCas9-mediated targeting of Ezh2 or UTX to the *DPYD* promoter (Figure 6).

In this manuscript, we identified the PU.1 transcription factor as an activator of *DPYD* expression (Figure 5). PU.1 is generally thought to regulate gene expression in circulating cells (40), but has also been identified as a metastatic suppressor in hepatocellular carcinoma (41). PU.1 has also been suggested to be involved in osteoclast development, adipogenesis, and aberrant Notch1 signaling linked to infertility (42–44). In the present study, we observed a positive correlation between *DPYD* and *SPI1* expression in RNA-seq data from TCGA datasets (Figure 5B) and in volunteer PBMCs (Figure 7L and 7M). These correlations, together with the observed reduction in *DPYD* after PU.1 knockdown (Figure 5C) and PU.1 enrichment on the *DPYD* promoter (Figure S4B) strongly indicate that PU.1 may be a key transcription factor that promotes *DPYD* expression in tumor and normal tissues.

In conclusion, understanding the mechanisms that contribute to drug sensitivity has the potential to significantly improve treatment planning decisions. Changes in the expression of genes related to drug metabolism could greatly affect tumor sensitivity to chemotherapy. In this manuscript we present a novel epigenetic mechanism of *DPYD* regulation and identify potential biomarkers that may be clinically useful in identifying patients who may benefit from aggressive adjuvant chemotherapy.

Supplementary Material

Refer to Web version on PubMed Central for supplementary material.

Acknowledgments

We thank Dr. Zhiguo Zhang for the histone H3 antibody, wildtype and K27M mutant plasmids, and for insightful discussions concerning dCas9-Ezh2 plasmid construction. The results shown here are in part based upon data generated by the TCGA Research Network: http://cancergenome.nih.gov/. We thank the Mayo Clinic Center for Individualized Medicine for the use of healthy volunteer samples from the Biobank and the Mayo Clinic Cancer Center for supporting additional shared resources (NIH CA 15083).

Financial support: NIH 5P30CA015083-42 (R.B.D.)

Reference

1. Carethers JM. Systemic treatment of advanced colorectal cancer: tailoring therapy to the tumor. Therap Adv Gastroenterol. 2008; 1:33–42.
2. Graham JS, Cassidy J. Adjuvant therapy in colon cancer. Expert Rev Anticancer Ther. 2012; 12:99–109. [PubMed: 22149436]
3. Lee AM, Shi Q, Pavey E, Alberts SR, Sargent DJ, Sinicrope FA, et al. DPYD variants as predictors of 5-fluorouracil toxicity in adjuvant colon cancer treatment (NCCTG N0147). J Natl Cancer Inst. 2014; 106
4. Heggie GD, Sommadossi JP, Cross DS, Huster WJ, Diasio RB. Clinical pharmacokinetics of 5-fluorouracil and its metabolites in plasma, urine, and bile. Cancer Res. 1987; 47:2203–2206. [PubMed: 3829006]

5. Offer SM, Wegner NJ, Fossum C, Wang K, Diasio RB. Phenotypic profiling of DPYD variations relevant to 5-fluorouracil sensitivity using real-time cellular analysis and in vitro measurement of enzyme activity. Cancer Res. 2013; 73:1958–1968. [PubMed: 23328581]
6. Caudle KE, Thorn CF, Klein TE, Swen JJ, McLeod HL, Diasio RB, et al. Clinical Pharmacogenetics Implementation Consortium guidelines for dihydropyrimidine dehydrogenase genotype and fluoropyrimidine dosing. Clin Pharmacol Ther. 2013; 94:640–645. [PubMed: 23988873]
7. Lee AM, Shi Q, Alberts SR, Sargent DJ, Sinicrope FA, Berenberg JL, et al. Association between DPYD c.1129–5923 C>G/hapB3 and severe toxicity to 5-fluorouracil-based chemotherapy in stage III colon cancer patients: NCCTG N0147 (Alliance). Pharmacogenet Genomics. 2015
8. Rosmarin D, Palles C, Pagnamenta A, Kaur K, Pita G, Martin M, et al. A candidate gene study of capecitabine-related toxicity in colorectal cancer identifies new toxicity variants at DPYD and a putative role for ENOSF1 rather than TYMS. Gut. 2015; 64:111–120. [PubMed: 24647007]
9. Salonga D, Danenberg KD, Johnson M, Metzger R, Groshen S, Tsao-Wei DD, et al. Colorectal tumors responding to 5-fluorouracil have low gene expression levels of dihydropyrimidine dehydrogenase, thymidylate synthase, and thymidine phosphorylase. Clin Cancer Res. 2000; 6:1322–1327. [PubMed: 10778957]
10. Fujiwara H, Terashima M, Irinoda T, Takagane A, Abe K, Kashiwaba M, et al. Quantitative measurement of thymidylate synthase and dihydropyrimidine dehydrogenase mRNA level in gastric cancer by real-time RT-PCR. Jpn J Cancer Res. 2002; 93:1342–1350. [PubMed: 12495474]
11. Ichikawa W, Uetake H, Shirota Y, Yamada H, Nishi N, Nihei Z, et al. Combination of Dihydropyrimidine Dehydrogenase and Thymidylate Synthase Gene Expressions in Primary Tumors as Predictive Parameters for the Efficacy of Fluoropyrimidine-based Chemotherapy for Metastatic Colorectal Cancer. Clinical Cancer Research. 2003; 9:786–791. [PubMed: 12576451]
12. Jenuwein T, Allis CD. Translating the histone code. Science. 2001; 293:1074–1080. [PubMed: 11498575]
13. Dawson MA, Kouzarides T. Cancer epigenetics: from mechanism to therapy. Cell. 2012; 150:12–27. [PubMed: 22770212]
14. van Haaften G, Dalgliesh GL, Davies H, Chen L, Bignell G, Greenman C, et al. Somatic mutations of the histone H3K27 demethylase gene UTX in human cancer. Nat Genet. 2009; 41:521–523. [PubMed: 19330029]
15. Hock H. A complex Polycomb issue: the two faces of EZH2 in cancer. Genes Dev. 2012; 26:751–755. [PubMed: 22508723]
16. Chan KM, Fang D, Gan H, Hashizume R, Yu C, Schroeder M, et al. The histone H3.3K27M mutation in pediatric glioma reprograms H3K27 methylation and gene expression. Genes Dev. 2013; 27:985–990. [PubMed: 23603901]
17. Olson JE, Ryu E, Johnson KJ, Koenig BA, Maschke KJ, Morrisette JA, et al. The Mayo Clinic Biobank: a building block for individualized medicine. Mayo Clin Proc. 2013; 88:952–962. [PubMed: 24001487]
18. Offer SM, Diasio RB. Response to "A case of 5-FU-related severe toxicity associated with the P.Y186C DPYD variant". Clin Pharmacol Ther. 2014; 95:137. [PubMed: 24107927]
19. Farre D, Roset R, Huerta M, Adsuara JE, Rosello L, Alba MM, et al. Identification of patterns in biological sequences at the ALGGEN server: PROMO and MALGEN. Nucleic Acids Res. 2003; 31:3651–3653. [PubMed: 12824386]
20. McCabe MT, Ott HM, Ganji G, Korenchuk S, Thompson C, Van Aller GS, et al. EZH2 inhibition as a therapeutic strategy for lymphoma with EZH2-activating mutations. Nature. 2012; 492:108–112. [PubMed: 23051747]
21. Schwartzentruber J, Korshunov A, Liu XY, Jones DT, Pfaff E, Jacob K, et al. Driver mutations in histone H3.3 and chromatin remodelling genes in paediatric glioblastoma. Nature. 2012; 482:226–231. [PubMed: 22286061]
22. Sturm D, Witt H, Hovestadt V, Khuong-Quang DA, Jones DT, Konermann C, et al. Hotspot mutations in H3F3A and IDH1 define distinct epigenetic and biological subgroups of glioblastoma. Cancer Cell. 2012; 22:425–437. [PubMed: 23079654]

23. Lewis PW, Muller MM, Koletsky MS, Cordero F, Lin S, Banaszynski LA, et al. Inhibition of PRC2 activity by a gain-of-function H3 mutation found in pediatric glioblastoma. Science. 2013; 340:857–861. [PubMed: 23539183]
24. Bender S, Tang Y, Lindroth AM, Hovestadt V, Jones DT, Kool M, et al. Reduced H3K27me3 and DNA hypomethylation are major drivers of gene expression in K27M mutant pediatric high-grade gliomas. Cancer Cell. 2013; 24:660–672. [PubMed: 24183680]
25. Lecomte T, Ferraz JM, Zinzindohoue F, Loriot MA, Tregouet DA, Landi B, et al. Thymidylate synthase gene polymorphism predicts toxicity in colorectal cancer patients receiving 5-fluorouracil-based chemotherapy. Clin Cancer Res. 2004; 10:5880–5888. [PubMed: 15355920]
26. Agger K, Cloos PA, Christensen J, Pasini D, Rose S, Rappsilber J, et al. UTX and JMJD3 are histone H3K27 demethylases involved in HOX gene regulation and development. Nature. 2007; 449:731–734. [PubMed: 17713478]
27. Hashizume R, Andor N, Ihara Y, Lerner R, Gan H, Chen X, et al. Pharmacologic inhibition of histone demethylation as a therapy for pediatric brainstem glioma. Nat Med. 2014; 20:1394–1396. [PubMed: 25401693]
28. Marisa L, de Reynies A, Duval A, Selves J, Gaub MP, Vescovo L, et al. Gene expression classification of colon cancer into molecular subtypes: characterization, validation, and prognostic value. PLoS Med. 2013; 10:e1001453. [PubMed: 23700391]
29. Dienstmann R, Salazar R, Tabernero J. Personalizing colon cancer adjuvant therapy: selecting optimal treatments for individual patients. J Clin Oncol. 2015; 33:1787–1796. [PubMed: 25918287]
30. Siegel RL, Miller KD, Jemal A. Cancer statistics, 2016. CA Cancer J Clin. 2016; 66:7–30. [PubMed: 26742998]
31. Fluge O, Gravdal K, Carlsen E, Vonen B, Kjellevold K, Refsum S, et al. Expression of EZH2 and Ki-67 in colorectal cancer and associations with treatment response and prognosis. Br J Cancer. 2009; 101:1282–1289. [PubMed: 19773751]
32. Ntziachristos P, Tsirigos A, Welstead GG, Trimarchi T, Bakogianni S, Xu L, et al. Contrasting roles of histone 3 lysine 27 demethylases in acute lymphoblastic leukaemia. Nature. 2014; 514:513–517. [PubMed: 25132549]
33. Xu B, On DM, Ma A, Parton T, Konze KD, Pattenden SG, et al. Selective inhibition of EZH2 and EZH1 enzymatic activity by a small molecule suppresses MLL-rearranged leukemia. Blood. 2015; 125:346–357. [PubMed: 25395428]
34. Zhou J, Bi C, Cheong LL, Mahara S, Liu SC, Tay KG, et al. The histone methyltransferase inhibitor, DZNep, up-regulates TXNIP, increases ROS production, and targets leukemia cells in AML. Blood. 2011; 118:2830–2839. [PubMed: 21734239]
35. Zhang Y, Liu G, Lin C, Liao G, Tang B. Silencing the EZH2 gene by RNA interference reverses the drug resistance of human hepatic multidrug-resistant cancer cells to 5-Fu. Life Sci. 2013; 92:896–902. [PubMed: 23562851]
36. Fan TY, Wang H, Xiang P, Liu YW, Li HZ, Lei BX, et al. Inhibition of EZH2 reverses chemotherapeutic drug TMZ chemosensitivity in glioblastoma. Int J Clin Exp Pathol. 2014; 7:6662–6670. [PubMed: 25400745]
37. Rizzo S, Hersey JM, Mellor P, Dai W, Santos-Silva A, Liber D, et al. Ovarian cancer stem cell-like side populations are enriched following chemotherapy and overexpress EZH2. Mol Cancer Ther. 2011; 10:325–335. [PubMed: 21216927]
38. Fillmore CM, Xu C, Desai PT, Berry JM, Rowbotham SP, Lin YJ, et al. EZH2 inhibition sensitizes BRG1 and EGFR mutant lung tumours to TopoII inhibitors. Nature. 2015; 520:239–242. [PubMed: 25629630]
39. Li Z, Wang Y, Qiu J, Li Q, Yuan C, Zhang W, et al. The polycomb group protein EZH2 is a novel therapeutic target in tongue cancer. Oncotarget. 2013; 4:2532–2549. [PubMed: 24345883]
40. Scott EW, Simon MC, Anastasi J, Singh H. Requirement of transcription factor PU.1 in the development of multiple hematopoietic lineages. Science. 1994; 265:1573–1577. [PubMed: 8079170]

41. Song LJ, Zhang WJ, Chang ZW, Pan YF, Zong H, Fan QX, et al. PU.1 Is Identified as a Novel Metastasis Suppressor in Hepatocellular Carcinoma Regulating the miR-615-5p/IGF2 Axis. Asian Pac J Cancer Prev. 2015; 16:3667–3671. [PubMed: 25987019]

42. Su RW, Strug MR, Jeong JW, Miele L, Fazleabas AT. Aberrant activation of canonical Notch1 signaling in the mouse uterus decreases progesterone receptor by hypermethylation and leads to infertility. Proc Natl Acad Sci U S A. 2016; 113:2300–2305. [PubMed: 26858409]

43. Wei N, Wang Y, Xu RX, Wang GQ, Xiong Y, Yu TY, et al. PU.1 antisense lncRNA against its mRNA translation promotes adipogenesis in porcine preadipocytes. Anim Genet. 2015; 46:133–140. [PubMed: 25691151]

44. Ishiyama K, Yashiro T, Nakano N, Kasakura K, Miura R, Hara M, et al. Involvement of PU.1 in NFATc1 promoter function in osteoclast development. Allergol Int. 2015; 64:241–247. [PubMed: 26117255]

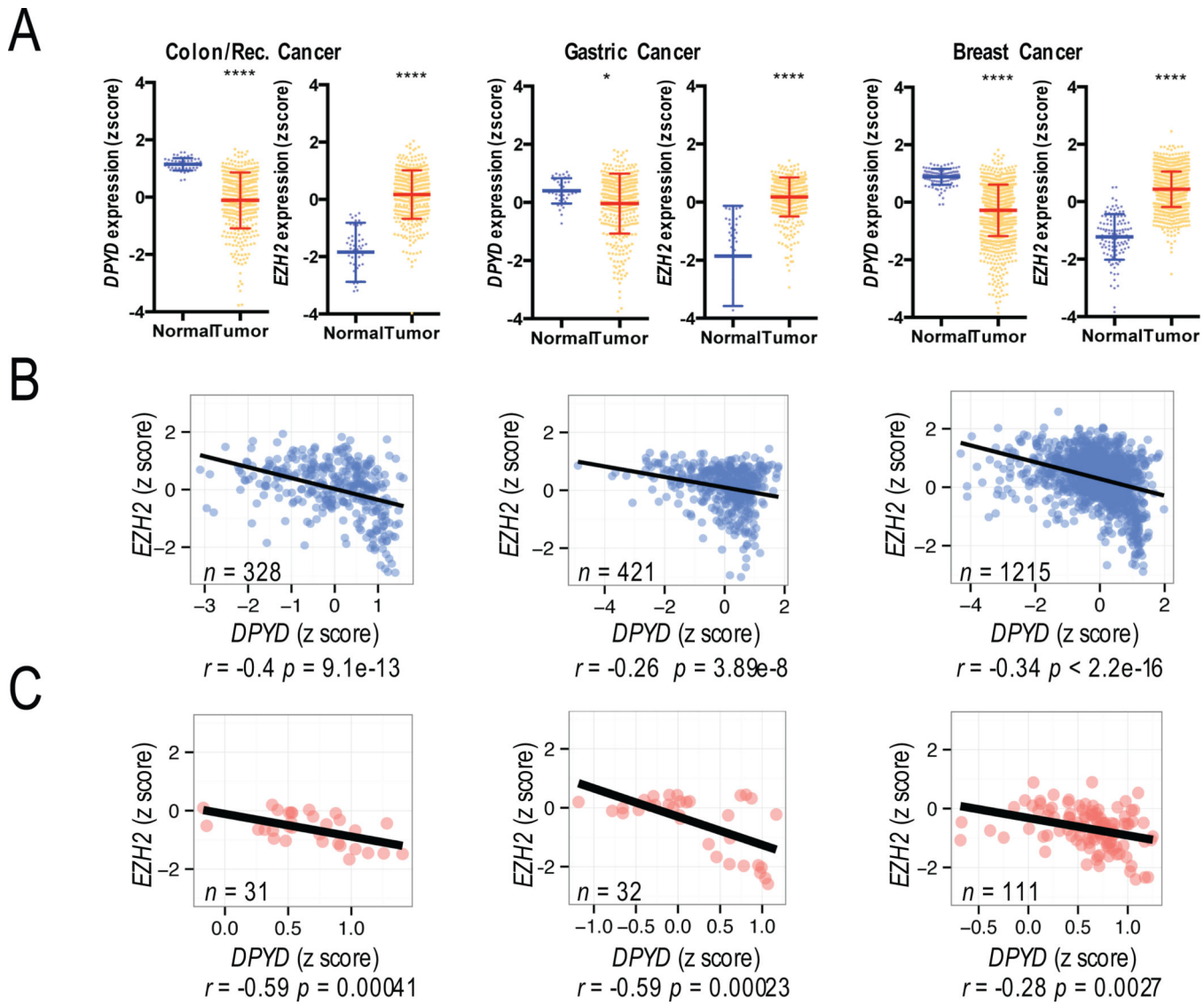

Figure 1. Relationship between *DPYD* and *EZH2* expression

A. Expression of *DPYD* and *EZH2* in tumor and normal tissues was compared in TCGA datasets for colon/rectum, gastric, and breast cancer. Plots represent the z-scores for log2-transformed normalized RNA-seq read counts. The calculated means +/− SD are represented by bars and whiskers. **B**. The correlations between *DPYD* and *EZH2* are presented for colon/rectum, gastric, and breast cancers. **C**. The correlations between *DPYD* and *EZH2* expression in normal tissue adjacent to colon/rectum, gastric, and breast cancers are shown. * p<0.05; **** p<0.0001

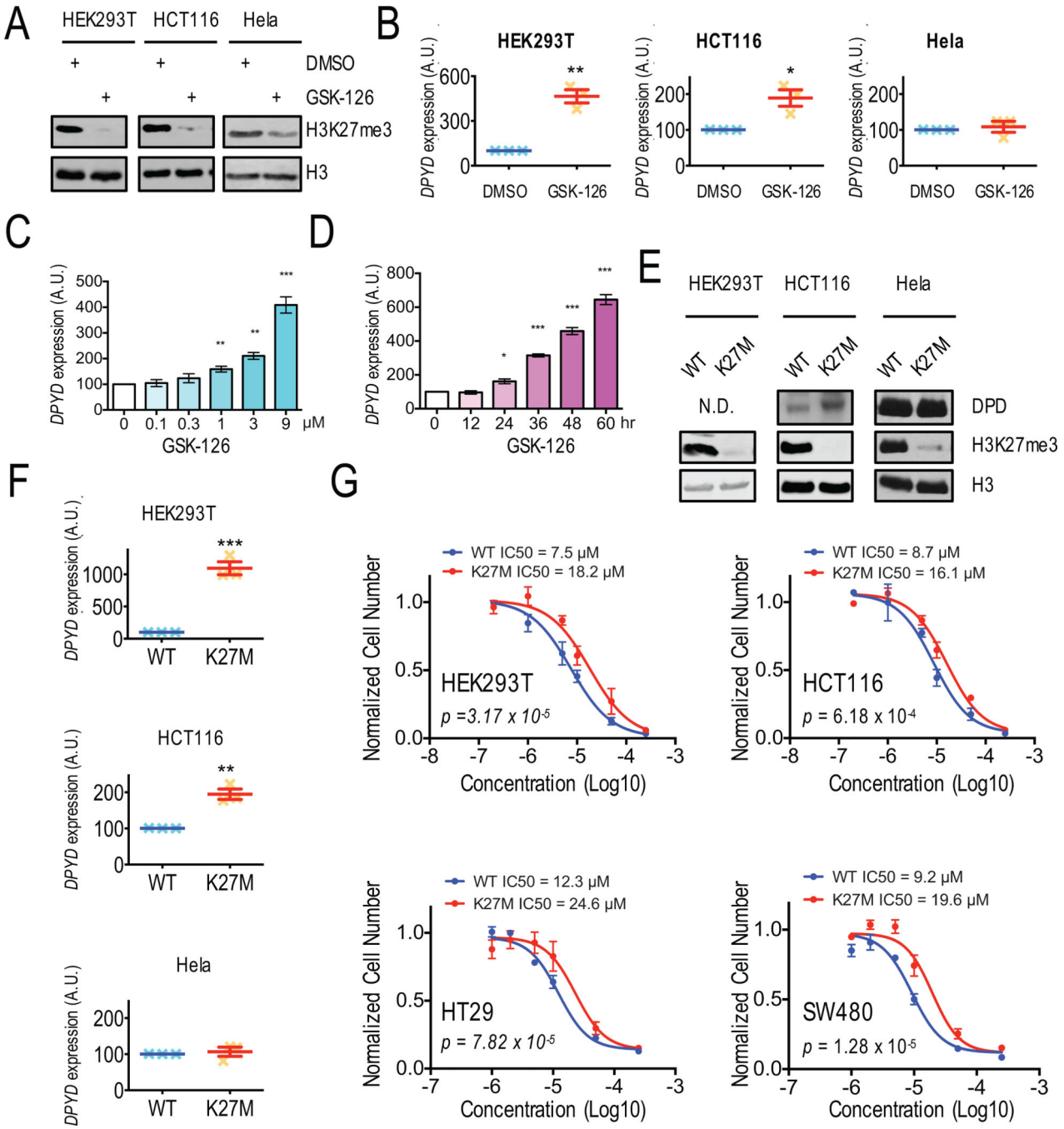

Figure 2. Inhibition of Ezh2 results in increased *DPYD* expression and desensitizes cells to 5-FU

A. Western blotting was used to measure histone H3 and H3K27me3 levels in HEK293T, HCT116, and Hela cells treated with DMSO or 1 μM GSK-126. **B**. *DPYD* expression in cells from (A) was measured by q-RT-PCR. **C**. *DPYD* expression was measured in HEK293T cells treated with the indicated concentrations of GSK-126. **D**. *DPYD* expression in HEK293T cells was measured at indicated time points following treatment with 1 μM GSK-126. **E**. DPD, H3K27me3, and total H3 expression in HEK293T, HCT116 and Hela cells stably expressing wild-type H3 and H3K27M were measured by western blotting. **F**.

DPYD expression was measured in cells from (E). **G**. IC_{50} concentrations for 5-FU were determined using HEK293T, HCT116, HT29 and SW480 cells stably expressing wild-type H3 (WT) or H3K27M (K27M). In all panels means +/− SD are represented by bars and whiskers. N.D., not detectable; * $p<0.05$; ** $p<0.01$; *** $p<0.001$; N.D. not detectable.

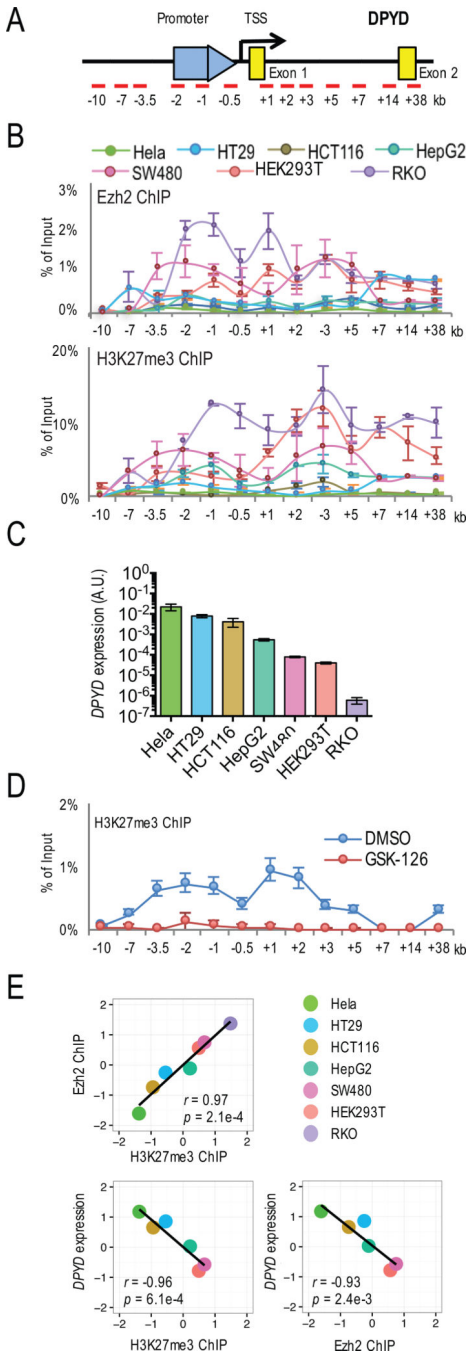

Figure 3. Enrichment of H3K27me3 and Ezh2 on the *DPYD* promoter and effect on *DPYD* expression

A. Schematic of the qPCR primer placement relative to the *DPYD* promoter, TSS, and first two exons is presented. **B**. Ezh2- (upper panel) and H3K27me3- (lower panel) associated genomic DNA from the indicated cell lines was obtained by chromatin immuno-precipitation (ChIP) and the enrichment at specific genomic regions was quantified by qPCR using primers indicated in (A). **C.** *DPYD* expression in Hela, HT29, HCT116, HepG2, SW480, HEK293T and RKO cells was measured. **D**. H3K27me3 enrichment was measured

by qPCR using ChIP DNA from HCT116 cells treated with 1 μM GSK-126 or DMSO. **E**. Pearson's correlation coefficients were calculated for *DPYD*, Ezh2 enrichment and H3K27me3 enrichment at the *DPYD* promoter using the sum of relative ChIP enrichment at −2 kb, −1 kb, −0.5 kb and +1 kb. *DPYD* mRNA and ChIP enrichment level were log2 transformed and standardized to z score.

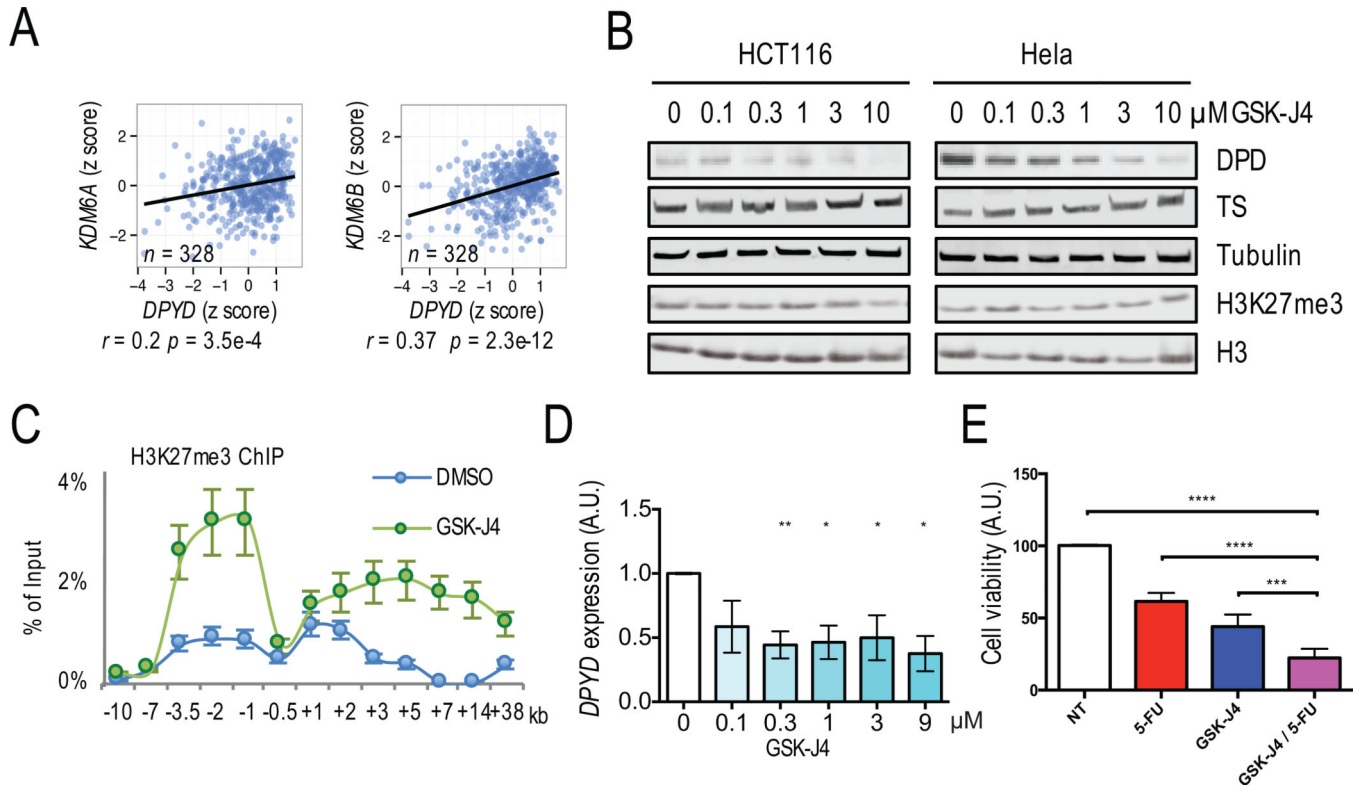

Figure 4. H3K27me3 demethylases UTX and Jmjd3 regulated *DPYD* expression

A. Correlations between *DPYD* and *UTX* (left panel) or *JMJD3* (right panel) expression were determined using normalized RNA read counts. **B**. Whole cell lysates from HCT116 and Hela cells treated with the indicated concentrations of GSK-J4 were immunoblotted using the indicated antibodies. **C**. H3K27me3 was immunoprecipitated from HCT116 cells treated with 1 μM GSK-J4 or DMSO control and analyzed by qPCR. **D**. Expression of *DPYD* was measured in cells from (B). **E**. The viability of HCT116 cultures treated with 5-FU, GSK-J4, 5-FU/GSK-J4 combination, or non-treated control (NT) was measured by realtime cell analysis. In all panels means +/− SD are represented by bars and whiskers. * p<0.05; ** p<0.01; *** p<0.001; **** p<0.0001

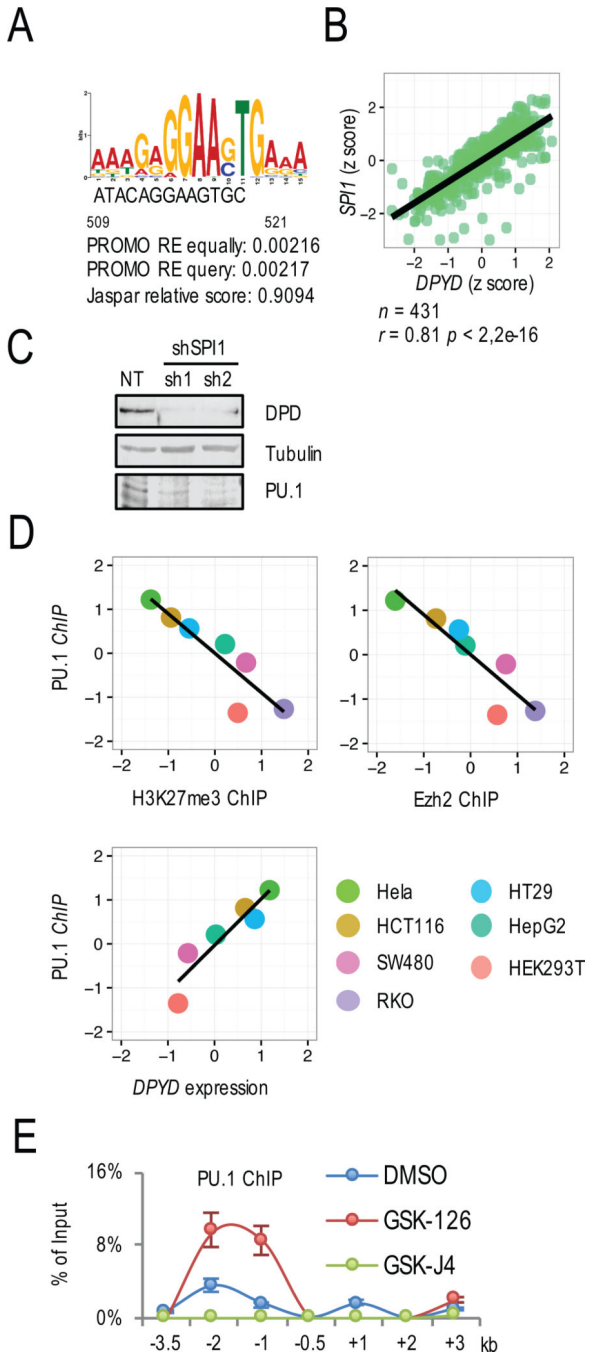

Figure 5. H3K27 trimethylation prevented PU.1 binding at the *DPYD* promoter

A. The PU.1 binding site was identified on the *DPYD* promoter located 509–521 nucleotide upstream from the TSS using PROMO. **B**. Correlation between *DPYD* and *SPI1* expression was determined in colon/rectum cancer TCGA data. **C**. DPD and PU.1 expression were measured by western blotting of HCT116 cells treated with two different shRNAs directed at PU.1 (sh1 and sh2) or non-target control shRNA (NT). **D**. Correlations between PU.1 and H3K27me3 enrichment at the *DPYD* promoter (top left), PU.1 and Ezh2 enrichment at the *DPYD* promoter (top right), and PU.1 and *DPYD* mRNA (bottom left) were determined for

cell lines indicated (bottom right). Cumulative ChIP enrichment was calculated as in Figure 3E. **E**. Changes in PU.1 enrichment at the indicated positions (relative to *DPYD* TSS as indicated) were determined by ChIP-qPCR from HCT116 cells treated with 1 μM GSK-126, 1 μM GSK-J4, or DMSO control.

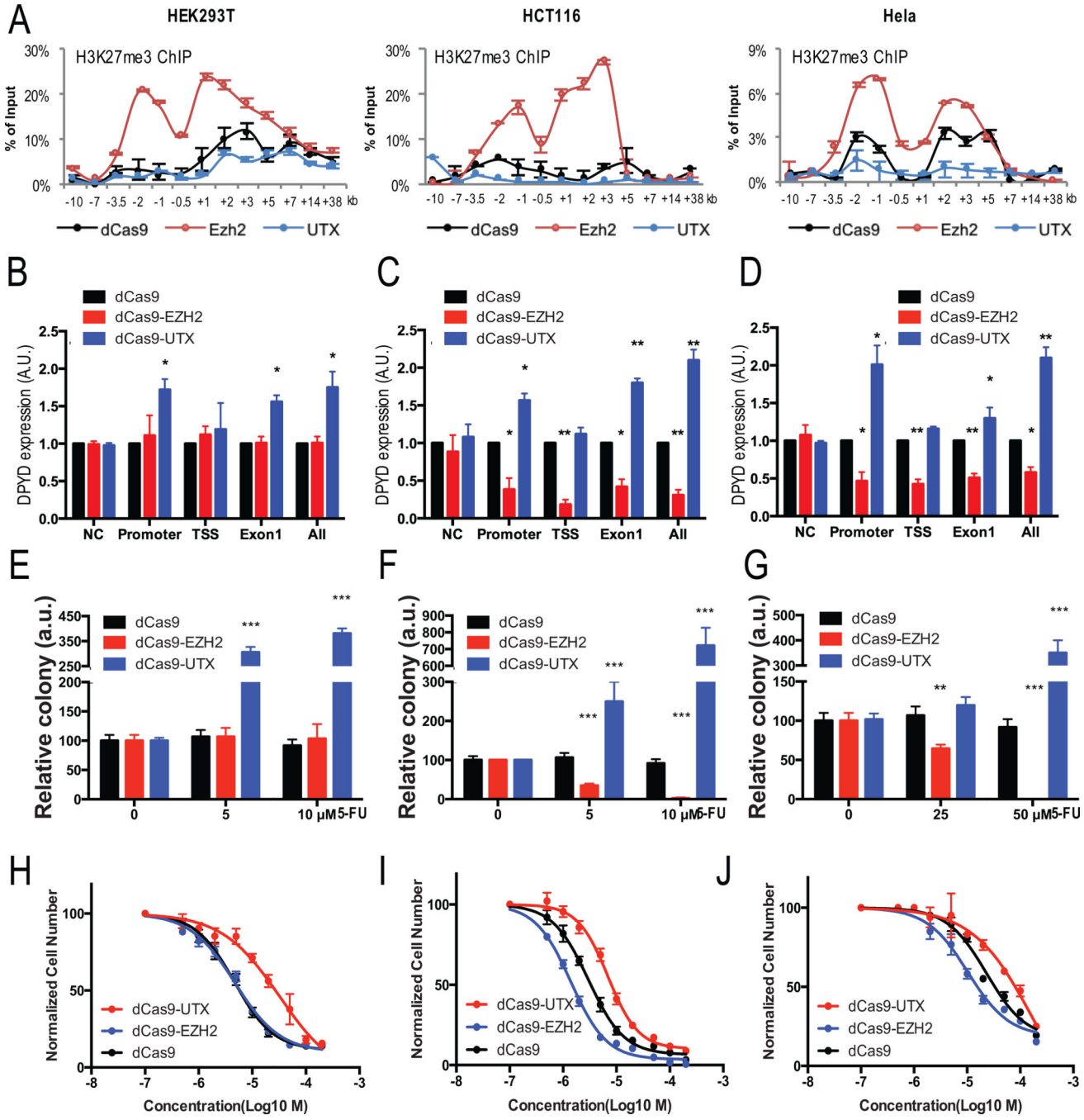

Figure 6. Regulating H3K27me3 specifically at the *DPYD* promoter changed *DPYD* expression and affected 5-FU sensitivity

A. H3K27me3 enrichment at the indicated regions (relative to *DPYD* TSS) was measured by ChIP-qPCR in HEK293T (left), HCT116 (center), and Hela (right) cells expressing dCas9 (control), dCas9-Ezh2, or dCas9-UTX and gRNAs targeting the promoter, TSS and 1st exon (see Figure S5A for the location of gRNA targets). **B–D**. *DPYD* expression was measured in HEK293T (B), HCT116 (C), and Hela (D) cells expressing dCas9, dCas9-Ezh2 or dCas9-UTX and gRNA targeting indicated positions. **E–G**. HEK293T (E), HCT116 (F), and Hela

(G) cells co-expressing gRNAs targeting promoter and the indicated dCas9 constructs were treated with the indicated concentration of 5-FU. Colonies were counted after four weeks. **H–J**. IC_{50} values for 5-FU were calculated for HEK293T (H), HCT116 (I), and Hela (J) cells co-expressing gRNAs targeting promoter. In all panels means +/− SD are represented by bars and whiskers. * $p<0.05$; ** $p<0.01$; *** $p<0.001$.

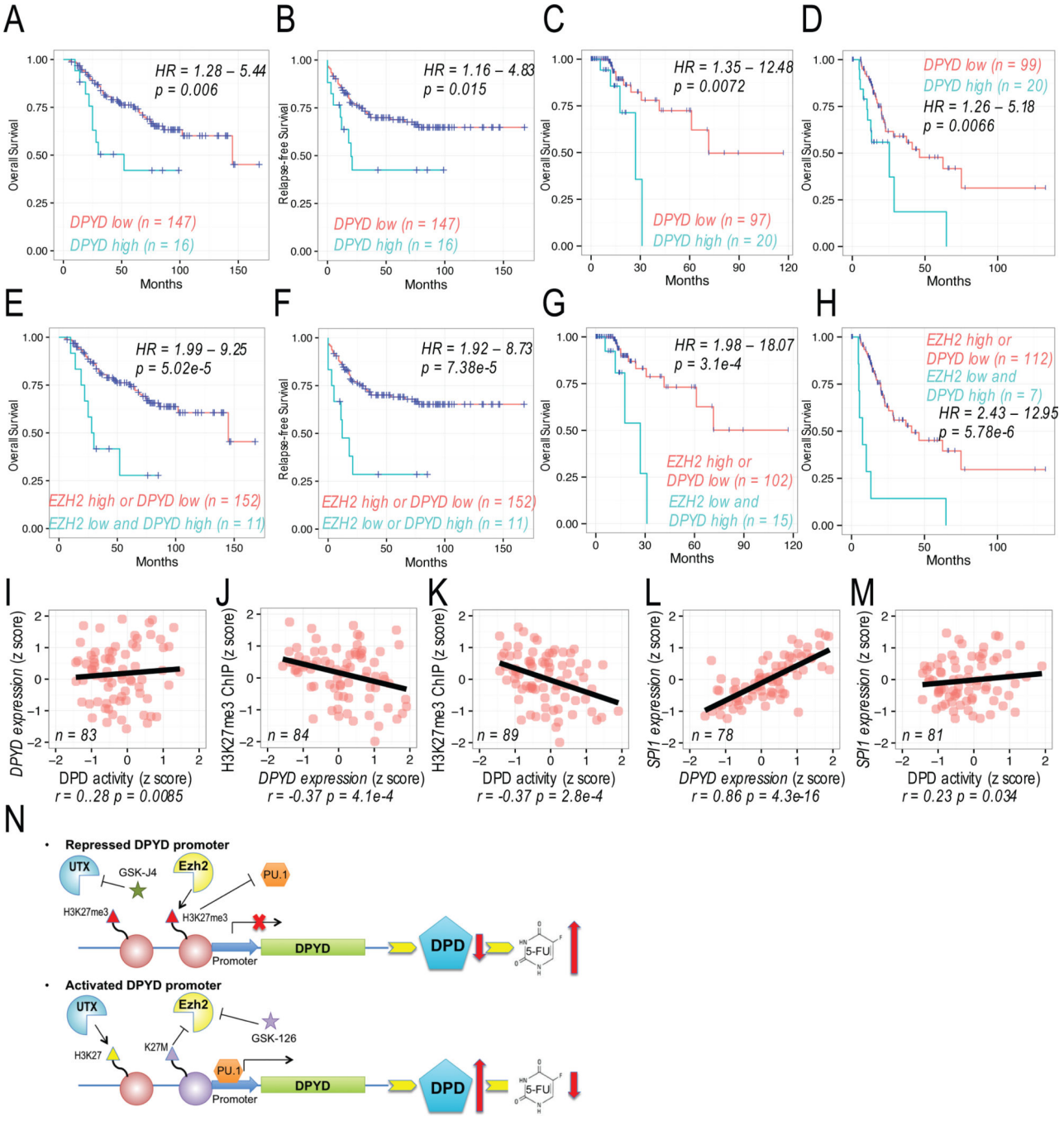

Figure 7. Role of Ezh2 in predicting *DPYD* expression and 5-FU response

A–B. Overall survival (A) and relapse-free survival (B) were determined for 5-FU treated colon/rectal cancer patients in GSE40967 dataset stratified by *DPYD* expression. **C–D** Overall survival was determined for 5-FU treated colon/rectal cancer (C) and gastric cancer (D) in TCGA dataset. **E–F**. Overall survival (E) and relapse-free survival (F) were determined for 5-FU treated colon/rectal cancer patients stratified by *DPYD* and EZH2 expression level as indicated. **G–H** Overall survival was determined for 5-FU treated colon/rectal cancer (G) and gastric cancer (H) patients stratified by *DPYD* and EZH2 expression

levels as indicated. **I–M**. Pearson's correlations were determined for DPD activity, *DPYD* expression, H3K27me3 enrichment on the *DPYD* promoter, and *SPI1* expression in peripheral mononuclear cells from healthy volunteers. **N**. A model of epigenetic regulation of the DPYD promoter and PU.1 accessibility is shown together with the effect on DPD expression and resultant 5-FU catabolism.